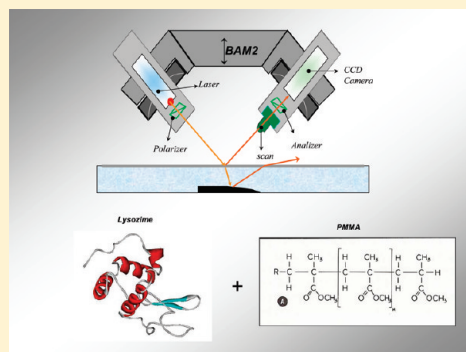


Interactions in Monolayers: A Study of the Behavior of Poly(methyl methacrylate)–Lysozyme Mixed Films from Surface Pressure–Area and Ellipsometric Measurements

M. Minones Conde,[‡] O. Conde,[†] J. M. Trillo,[†] and J. Minones, Jr.*

[†]Department of Physical Chemistry, Faculty of Pharmacy and [‡]Department of Optometry, School of Optics and Optometry, University of Santiago de Compostela, Campus Sur., 15706-Santiago de Compostela, Spain

ABSTRACT: Mixed monolayers of PMMA–lysozyme show the existence of negative deviations from the additivity of the molecular areas (A_m) when the composition of polymer mixtures is less than $X_{\text{PMMA}} 0.6$, regardless of the surface pressure of the monolayers. The maximum deviation occurs in the mixed monolayer with composition $X_{\text{PMMA}} 0.25$, which is attributed to the formation of a complex consisting of one polymer molecule and three protein molecules (1:3 stoichiometry), stabilized by hydrogen bonds between the NH groups of the protein and the CO groups of the polymer as well as by van der Waals attractive forces between the hydrocarbon chains of both components. When the relative proportion of the components in the mixed films significantly differs from the value corresponding to the stoichiometry of the complex (as in mixtures with $X_{\text{PMMA}} > 0.6$), this complex cannot be formed, causing an immiscible system where the values of the experimental molecular areas coincide with those corresponding to ideal behavior. Measurements of monolayer thickness and BAM images allow confirmation on the microscopic level of the structural characteristics deduced from the π – A isotherms.



1. INTRODUCTION

The tear film is a liquid layer of a complex, dynamic, and changing structure covering the front surface of the eye. Although knowledge on tear film, including the influence exerted by contact lenses, is still scarce, it is known to play an important role in vision because it increases the resolution power of the eye as a result of the fact that it provides a smooth optical surface on the corneal epithelium, reducing its irregularity. Besides, it forms a barrier between the extraocular environment and the corneal–conjunctival surface, protecting the eye.

The aqueous layer of the tear film is made up mostly of the secretion of the main and accessory lacrimal glands and includes 98% of the total thickness of the film. It consists of a dilute aqueous solution containing inorganic electrolytes and soluble organic compounds, among which the most important are proteins, enzymes, and hormones. There are ~60 proteins, most of which have an isoelectric point between 4 and 6, and their molecular weights range from 14 000 to 400 000 g/mol, with an average value of 50 000 g/mol. The protein content of tears differs in many respects from that of blood,¹ its concentration being of 4–10 g/L, that is 10 to 15 times lower than in human serum. Among these proteins, lysozyme is one of the most important characteristics of the tear. It is a globular protein (isoelectric point, PI 11²), and its molecular weight is 14 300 g/mol,³ containing 129 amino acid residues.⁴ Its concentration in tears is higher than that in any other body fluids, being from 0.83 to 2.06 g/L,⁵ although this value, as well as that of other tear proteins, partially depends on the sample collection procedure.⁶

This concentration represents the 21–25% of total tear proteins, and it is reduced by the systemic administration of corticosteroids, glucose, urea, and insulin. In addition, it also decreases in polluted environments.⁷ By contrast, tear lysozyme content increases in the case of eye diseases, after drinking water, and after administration of epinephrine or histamine.

The bactericidal action of lysozyme is due to its ability to dissolve the bacterial cell membrane by enzymatic digestion. For a long time, it was thought that lysozyme was the only antimicrobial substance in tears. However, it is believed that this antibacterial activity is activated by the betalysin, although some authors doubt the existence of this compound in tears because it is mistaken with lactoferrin.² Lytic activity of lysozyme depends on the pH, with the optimal value ranging between 6 and 7.4; a low concentration of salts favors lysis by an increased protein solubility, and, on the contrary, certain chemical antiseptics are antagonists of lysozyme, reducing its antibacterial properties.

Currently, the correction of most eye refraction anomalies is carried out using contact lenses made of polymers with different composition, which, unlike conventional glasses, are in contact with the tear film, to which can be affected. For this reason, the materials used for contact or intraocular lenses must have proven safety and performance characteristics that make them compatible with the environment in which they are inserted, that is, the

Received: September 23, 2010

Revised: May 18, 2011

Published: May 23, 2011

eye and its parts: eyelids and tear film. It has to be transparent, nontoxic, resistant to deposition of tear film components, and durable; show good wettability and oxygen permeability; and provide proper optical correction but still be inexpensive.

Given all of this, the poly(methylmethacrylate) (PMMA) would be the material of choice, but it does not have the requirement of being permeable to gases (O_2 and CO_2). A material with good gas permeability and at the same time able to maintain its adequate mechanical strength and the dimensional stability required to ensure the optical correction during use has not yet been found. Therefore, for example, soft materials, which are more permeable to gases because of their water content, are more unstable to changes in pH and temperature because their hydration is increased, which favors the formation of deposits and a lower wettability.

In addition, the materials used in the manufacture of contact lenses should be resistant to protein deposition because their adsorption onto the lens surface causes loss of transparency; this phenomenon depends, on the one hand, on the individual response to the lenses and, on the other hand, on the hydrophilic nature of their surface. The hydrophilicity can be modified by inserting appropriate functional ionic or polar groups into the polymer structure, provided that these groups are not toxic to the user, or by applying some coatings as a thin film resistant to protein adhesion⁸ on the lens surface.

As explained above and given that, on the one hand, lysozyme is one of the main proteins of the tear responsible for the formation of deposits on contact lenses and, on the other hand, that the PMMA is one of the most common polymers used in the manufacture of these lenses, this work has been focused on the study of possible interactions that may occur between these two components, using the Langmuir monolayer technique, which has been found to be a very successful tool in examining interaction in biological systems.⁹ The analysis of surface pressure-area isotherms recorded as a consequence of the compression of mixed monolayers, together with ellipsometric measurements and Brewster angle microscopy observations (BAM), will allow us to determine the behavior and morphology of mixed monolayers, that is, whether there are any interactions between their components.

2. EXPERIMENTAL SECTION

2.1. Materials. Lysozyme from chicken egg white, crystallized, was supplied from Sigma (purity 95%) and stored according to the supplier information. The protein spreading solution was a mixture made of 0.5 M sodium acetate and propyl alcohol in 1:1 v/v proportion.¹⁰

Syndiotactic PMMA of molecular weight $M_w = 15\,000$ g/mol was purchased from Aldrich (purity 95%) and used without further purification. Stock solutions of 0.1 to 0.3 mg/mL concentration were prepared using chloroform as a solvent supplied by Merck (purity 99–99.4% GC). The polydispersity (M_w/M_n) of this PMMA was not measured because, according to other authors,^{11–14} the molecular weight distribution effect is believed to be minimal on the monolayers behavior.

2.2. Spreading of Materials. In the study of protein monolayers, the main problem that arises is to obtain a stable film because in most cases proteins are soluble in water and, accordingly, when trying to carry out their spreading over a water surface, they can cause losses as a result of their dissolution or desorption in the subphase. Different procedures have been

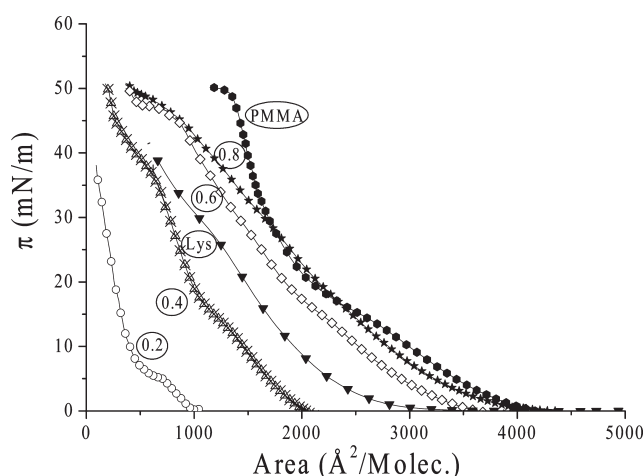


Figure 1. Surface pressure (π)–area (A) isotherms of PMMA–lysozyme mixed monolayers spread on aqueous substrate of NaCl 3 M (pH 10 to 11 at 30 °C).

devised to reduce or avoid losses. According to Trurnit,¹⁵ the most satisfactory procedure to ensure a proper spreading of the protein consists of applying the spreading solution to the top of a glass rod of 5 mm in diameter and 10 cm long, vertically placed in the trough containing the substrate. If the flow rate, protein concentration, length, and diameter of the rod are chosen properly, then protein molecules diffuse at the air/water interface along the rod and unfold so that upon arrival in this state to the surface of the water they do not dissolve and therefore become part of the monolayer. Results of Muratmasu and Sobotka¹⁶ confirm that this method leads to good spreading in the case of bovine serum albumin. The same happens to other proteins.^{17–20} Taking into account this background, the procedure we used for the spread of lysozyme was the Trurnit method. A substrate of high ionic strength (NaCl 3M) and a pH value near the isoelectric point of lysozyme (pH 10 to 11) was used in all experiments to reduce its solubility into the aqueous subphase.

Other factors that have an influence on the spreading of the protein, such as the elapsed time between the deposit of the film and the beginning of compression and the number of molecules deposited (i.e., the surface concentration of the protein, c_s) have been analyzed in a previous work,²¹ leading to the conclusion that the best extension conditions are achieved when the number of molecules deposited is 1×10^{15} ($c_s = 2.1 \text{ m}^2/\text{mg}$) and the waiting time is 3 h.

Ultrapure water used as subphase was obtained from a Milli-Ro, Milli-Q reverse osmosis system (Millipore) with a resistivity of 18.2 MΩ cm. The regulation of the trough temperature (30 °C) was controlled by circulating constant temperature water from Haake thermostat through the tubes attached to the aluminum-based plate of the trough. The subphase temperature was measured by a thermocouple located just below the air/water interface.

2.3. Surface Film Balance. Surface pressure–area isotherms of PMMA–lysozyme mixed films were recorded with a Nima Langmuir trough (total area = 490 cm²) placed on an isolated vibration-free table and enclosed in a glass chamber to avoid contamination from the air. A barrier confining the monolayer at the interface was driven at a constant speed of 36 cm²/min during the film compression. This is the highest value at which isotherms have been found to be reproducible in preliminary experiments.²²

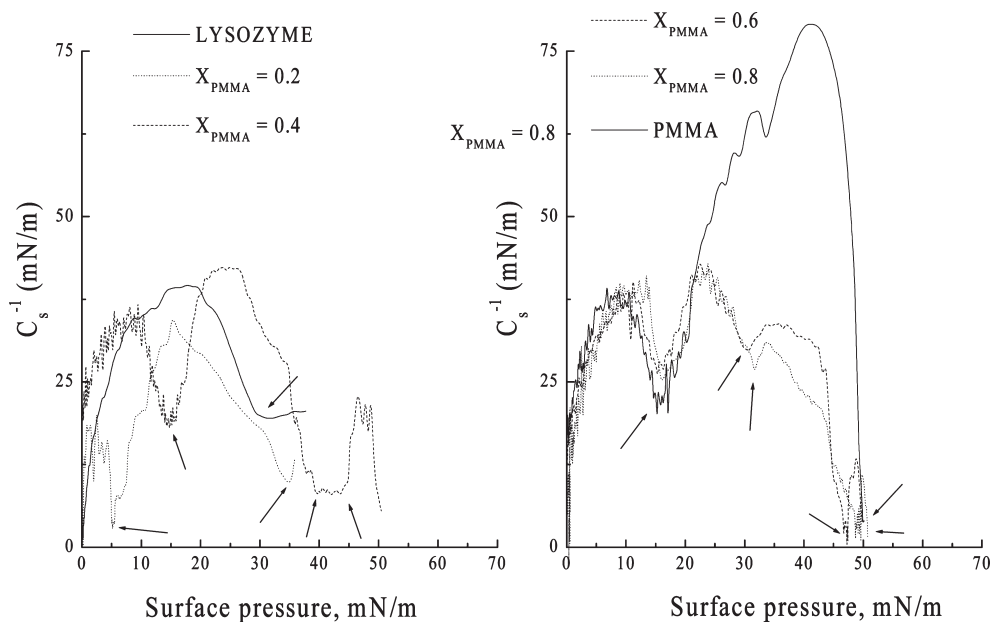


Figure 2. Compressional modulus (C_s^{-1})—surface pressure (π) plots for pure components and for mixed PMMA–lysozyme monolayers spread on aqueous substrate of NaCl 3 M (pH 10 to 11 at 30 °C). Arrows show the minima values corresponding to the LE–L'E phase transition of PMMA and to the collapses of lysozyme and PMMA monolayers.

Table 1. Compressional Modulus Values at Different Surface Pressures Together with Surface Pressures Corresponding to LE–L'E Phase Transition and to Collapses of PMMA–Lysozyme Mixed Monolayers

mole fraction of PMMA	compressional modulus C_s^{-1} (mN/m)			π_{trans}	π_{coll}
	at 5 mN/m	at 15 mN/m	at 30 mN/m		
0	26.6	39.1	19.8		31.0
0.2	15.0	29.0	39.4	5.1	35.0
0.4	32.5	19.0	38.7	14.5	38.2
0.6	31.1	28.0	31.5	15.6	30.5
0.8	33.5	32.7	39.7	15.8	31.0
1	36.0	22.6	61.0	15.6	47.4

Surface pressure was measured with the accuracy of ± 0.1 mN/m using a Wilhelmy plate made of chromatographic paper as a pressure sensor.

2.4. Brewster Angle Microscopy. BAM images and ellipsometric measurements were performed with BAM 2 Plus (NFT, Göttingen, Germany) equipped with a 30 mW laser emitting p-polarized light with a wavelength of 532 nm that was reflected off the air/water interface at $\sim 53.1^\circ$ (incident Brewster angle). Under such conditions, the reflectivity of the beam was almost zero on the clean water surface. The reflected beam passes through a focal lens into an analyzer at a known angle of incident polarization and finally to a CCD camera. For measurement of the relative thickness of the film, a camera calibration was previously necessary to determine the relationship between the gray level (GL) (intensity unit) and the relative reflectivity (I), according to the procedure described by Rodríguez Patino et al.²³ The light intensity at each point in the BAM image depends on the local thickness and the film optical properties. These parameters can be measured by determining the light intensity at the camera and analyzing the polarization state of the reflected light through the method based on Fresnel equations. At the Brewster

angle: $I = |R_p|^2 = Cd^2$, where I is the relative reflectivity (defined as the ratio of the reflected intensity (I_r) and the incident intensity (I_0), $I = I_r/I_0$), R_p is the p-component of the light, C is a constant, and d is the film thickness.

The lateral resolution of the microscope was $2 \mu\text{m}$, the shutter speed used was 1/50 s, and the images were digitized and processed to optimize image quality; those shown below correspond to 768×572 pixels.

3. RESULTS

3.1. Surface Pressure (π)–Area (A) Isotherms for Mixed Films of PMMA–Lysozyme. For the study of the interaction between these two components, 1×10^{15} molecules of lysozyme were spread using the Trurnit method on an aqueous substrate of high ionic strength (NaCl 3 M and pH 10 to 11 at 30 °C). In the Nima trough, a first compression and decompression of the monolayer was made, leaving it to stand for ~ 3 h to attain the unfolding of the protein amino acid chains; then, an appropriate amount of PMMA (molecular weight 15 000) was deposited for each mole fraction. Finally, the compression of

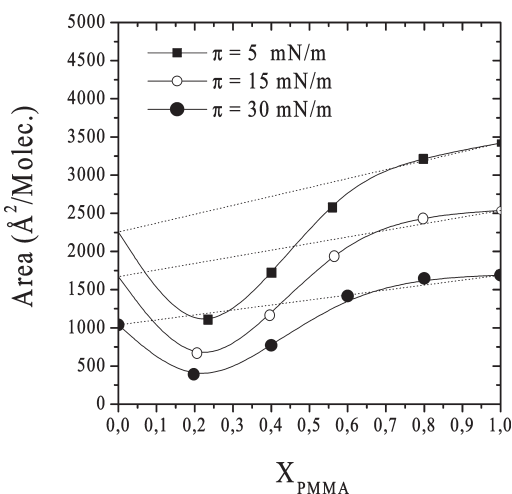


Figure 3. Mean molecular area versus mole fraction plots for PMMA–lysozyme mixed monolayers at different surface pressures. Dashed lines: ideal behavior. Solid lines: experimental results.

the lysozyme–PMMA mixed monolayer was carried out. The results can be seen in Figure 1. All mixed films show the characteristic LE–L'E phase transition of PMMA²² at surface pressure values ranging between 5 (mole fraction of PMMA, $X_{\text{PMMA}} = 0.2$) and 16 mN/m ($X_{\text{PMMA}} = 0.8$), where this transition is less clear. At surface pressure values ranging between 35 and 48 mN/m, the isotherms show a second plateau, which corresponds to the collapse of the films. For pure lysozyme, this collapse begins at much lower surface pressure values (~ 30 mN/m), and in the mixed film $X_{\text{PMMA}} = 0.2$, it is not visualized in the corresponding isotherm, although in the compressional modulus curve (which will be described in the following section), the existence of a minimum, relative to the monolayer collapse, can be observed.

The mixed film corresponding to $X_{\text{PMMA}} = 0.4$ has a clear collapse at 38 mN/m, and in the mixed films with composition $X_{\text{PMMA}} = 0.6$ and 0.8, it appears around 47.5 mN/m, this value matching the collapse surface pressure of pure PMMA under the working conditions used in this study.

In these mixtures, there is another collapse at surface pressures of ~ 30 mN/m, caused by the ejection of lysozyme molecules from the mixed monolayers, which cannot be seen in the corresponding isotherms displayed on a normal scale, but by extending them, it can be clearly observed. Both compressibility curves and BAM images will confirm the existence of this collapse.

One can see that not all isotherms of this mixed system are situated between those of pure components. So, the corresponding curves to $X_{\text{PMMA}} = 0.2$ and 0.4 mixed films are displaced to the left of both pure lysozyme and PMMA isotherms, whereas the compression curves of the remaining mixed monolayers are situated between those of pure components.

3.2. Compressional Modulus (C_s^{-1})–Surface Pressure (π) Curves. C_s^{-1} – π curves corresponding to pure and mixed monolayers of lysozyme and PMMA are shown in Figure 2. Curves relative to mixed monolayers exhibit two maxima values separated by a minimum point, characteristic of the LE–L'E phase transition of PMMA, as mentioned in the previous section. The first maximum appears at a surface pressure of ~ 10 mN/m, with a C_s^{-1} value of 35–37 mN/m, which is characteristic of liquid-expanded monolayers. The second maximum occurs at

surface pressures near 30 mN/m, with C_s^{-1} values ranging between 42 and 46 mN/m, also characteristic of a liquid expanded state.

In all curves, between both of the maxima values, the existence of a minimum point, which as just noted, corresponds to the LE–L'E phase transition of PMMA, can be observed. The compressional modulus corresponding to this minimum increases with the polymer content in the mixture. This is consistent with the fact that the plateau that appears in the π –A isotherms (corresponding to the phase transition) is less flat with increasing PMMA content.

Besides this minimum, the curves exhibit another minimum (or more) at higher surface pressures, which corresponds to the collapse (or collapses) of the mixed monolayers. Thus, in the mixed film of composition $X_{\text{PMMA}} = 0.2$, this second minimum is observed at a surface pressure of 35 mN/m, whereas for the PMMA mixture of $X_{\text{PMMA}} = 0.4$, the surface pressure at which it appears is somewhat higher, ranging between 40 and 44 mN/m (mean value, 42 mN/m), being therefore a region of minimum compressional modulus instead of a minimum point. This corresponds in the π –A isotherm to the existence of a “pseudo-plateau”, which continues as the monolayer is compressed (Figure 1).

The behavior of the mixed monolayers with composition $X_{\text{PMMA}} = 0.6$ and 0.8 is different from the one above because the compressional modulus curves show the existence of two minima values: one at a surface pressure of 30 mN/m (due to the collapse of lysozyme) and another at a surface pressure of ~ 47.5 mN/m, which is identified with the collapse of PMMA.

Table 1 shows LE–L'E phase transition values for the PMMA–lysozyme mixed system, together with compressional modulus at different surface pressures. The surface pressure (or pressures) corresponding to the collapses of the mixed monolayers are also included. In mixtures of composition $X_{\text{PMMA}} = 0.2$ and 0.4, there is only one value of this surface pressure as a result of the existence of a single collapse. However, the mixed monolayers with a composition of $X_{\text{PMMA}} = 0.6$ and 0.8 show two collapses corresponding to the ejection of each component from the mixed monolayer.

3.3. Mean Molecular Area versus Mole Fraction Plots. Undoubtedly, the mean molecular area–mole fraction plots provide better information to prove the existence (or not) of interactions between the components of the mixed monolayers, unlike the π –A isotherms, which only allow observation of the behavior of the monolayers with different composition, but they do not differentiate whether the components of a mixed film have greater or less interaction than those of another composition. Therefore, to obtain further information, we have proceeded to plot the mean molecular area occupied by the mixed films of lysozyme and PMMA as a function of the mole fraction of PMMA. The obtained results are shown in Figure 3 for substrates of ionic strength 3 (3 M NaCl) and pH 10 to 11 at 30 °C.

The existence of negative deviations from ideality in mixtures of polymer mole fraction <0.6 can be observed at all surface pressures studied: low, medium, and high. The maximum deviation occurs in the mixed monolayer with composition $X_{\text{PMMA}} \approx 0.25$. The observed negative deviations are characteristic of the molecular area contraction of the two-component film due to attractive interactions.^{24–26} When the mole fraction of PMMA is >0.6 , the experimental values (solid lines) coincide with those corresponding to the ideal behavior (dashed lines).

3.4. BAM Images and Thickness versus Surface Pressure Curves. In this section, we have first included the BAM images

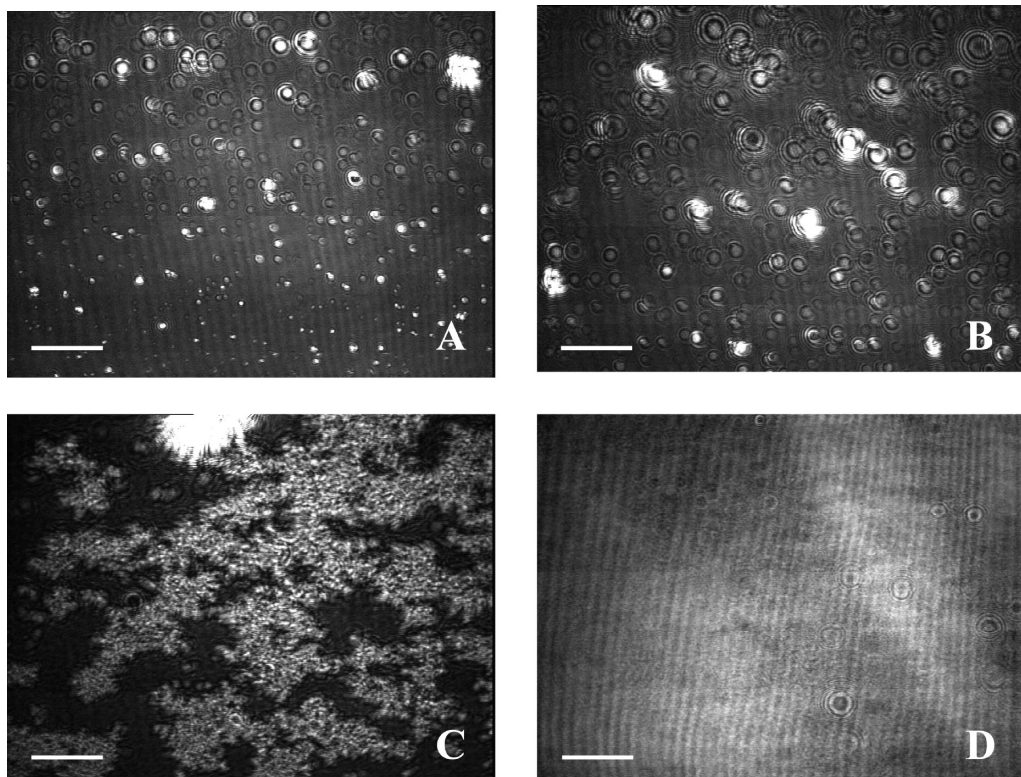


Figure 4. BAM images corresponding to lysozyme monolayer at different surface pressures: (A) $\pi = 14.3 \text{ mN/m}$. (B) $\pi = 23.5 \text{ mN/m}$. (C) $\pi = 39.4 \text{ mN/m}$. (D) $\pi = 47.3 \text{ mN/m}$. Scale bar: $20 \mu\text{m}$.

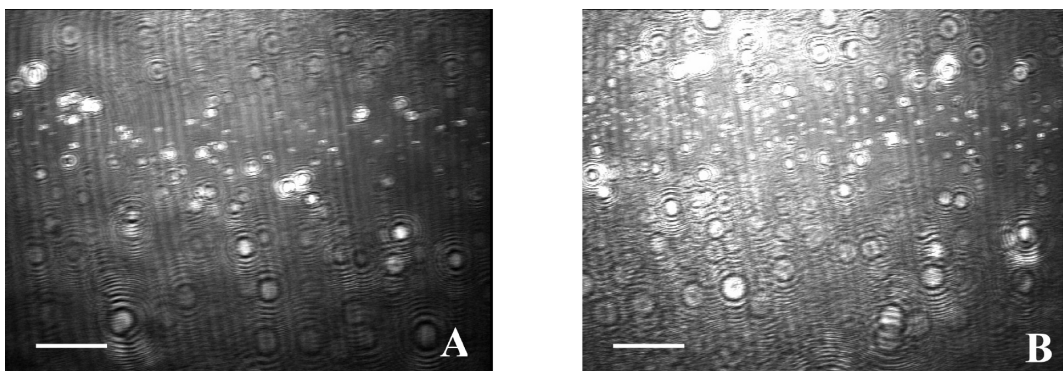


Figure 5. BAM images corresponding to PMMA monolayer at different surface pressures: (A) $\pi = 16.7 \text{ mN/m}$. (B) $\pi = 39 \text{ mN/m}$. Scale bar: $20 \mu\text{m}$.

corresponding to the microscopic observation of the lysozyme monolayer at different surface pressures (Figure 4) and those of PMMA (Figure 5), both spread on 3 M NaCl (pH 10 to 11, temperature 30°C), to compare these images with those corresponding to the mixtures. The evolution of the mixed monolayer thickness (d) with surface pressure (π) was analyzed, and its behavior was compared with that of the pure components.

Figure 4A was obtained when the surface pressure of the lysozyme monolayer was $\sim 14 \text{ mN/m}$, showing the existence of small condensation nuclei, which increase in size as the film is compressed (Figure 4B). When the monolayer begins to collapse, the presence of large aggregates, similar to clusters corresponding to residues of collapsed monolayer, becomes obvious (Figure 4C). At higher surface pressures

than 47 mN/m , the aggregates merge, resulting in thick homogeneous stripes (Figure 4D).

Figure 5 corresponds to BAM images of PMMA obtained at the surface pressure of 16.7 mN/m , showing small circular domains of great reflectivity (white circles) (Figure 5A), which are grouped with compression (Figure 5B).

3.4.1. Mixed Monolayer of $X_{\text{PMMA}} = 0.2$. Figure 6 shows that the mixed monolayer has a similar thickness to that of lysozyme and lower than that of the PMMA, with noise peaks like those of the protein. In the region of low surface pressures, the BAM image shows an almost homogeneous appearance, with limited presence of small circular domains (Figure 6A), which are responsible for the few noise peaks observed in this region. As the monolayer is compressed above 5 mN/m (corresponding to

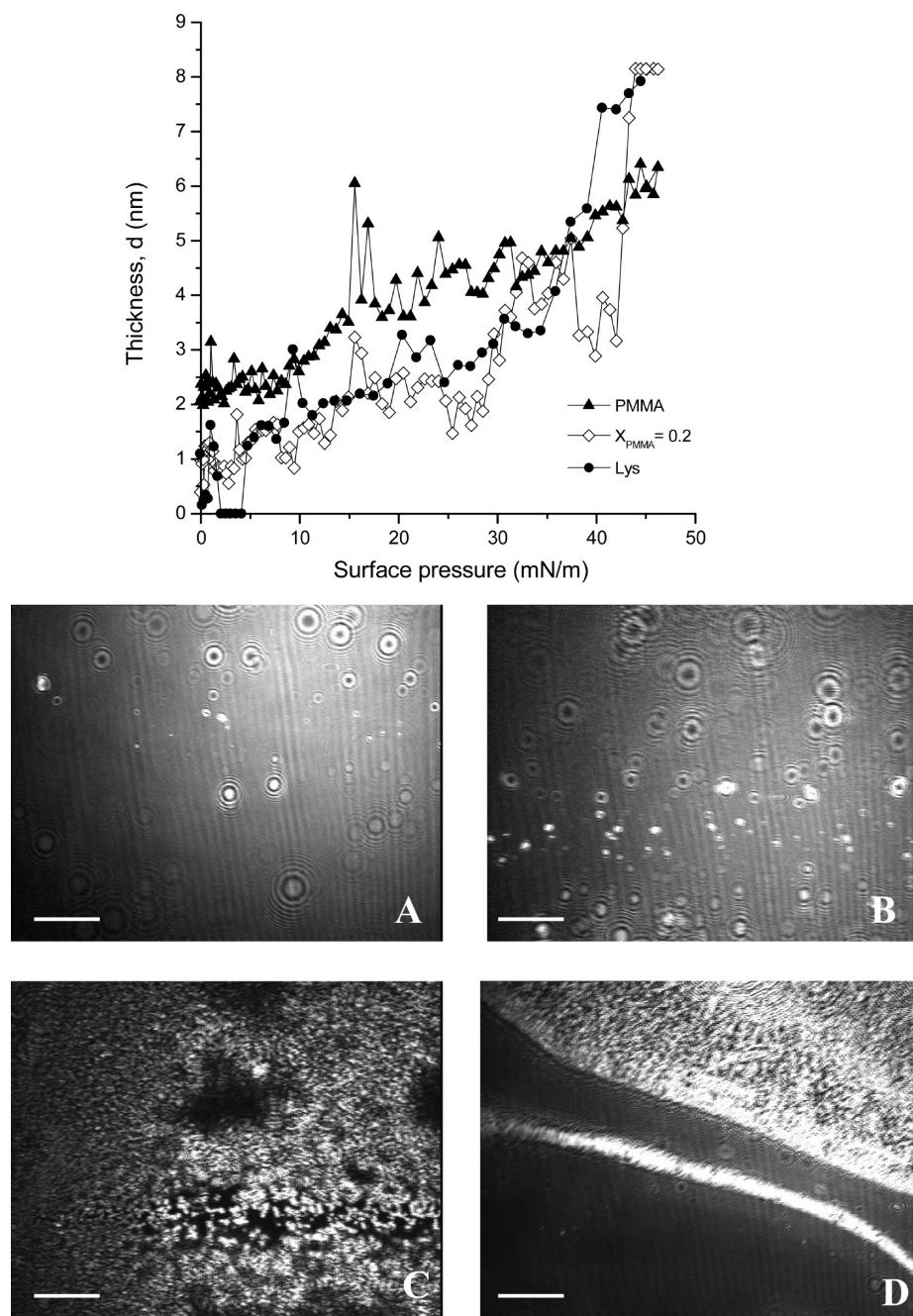


Figure 6. Thickness versus surface pressure plots corresponding to pure and PMMA–lysozyme mixed monolayer of composition $X_{\text{PMMA}} = 0.2$ and BAM images obtained at different surface pressure values: (A) $\pi = 2.9 \text{ mN/m}$. (B) $\pi = 25.2 \text{ mN/m}$. (C) $\pi = 32.2 \text{ mN/m}$. (D) At the end of compression. Scale bar: $20 \mu\text{m}$.

the surface pressure LE–L'E phase transition of PMMA), the film thickness is continuously increasing, showing the appearance of significant noise peaks due to the existence of numerous circular domains (Figure 6B), similar to those observed in pure lysozyme at surface pressures of 14 (Figure 4A) and 23 mN/m (Figure 4B). Under these conditions, the thickness curve practically coincides with that of the lysozyme, which is logical because of the high proportion of protein in the mixed film. In any case, further analysis shows that the curve for the mixture always has less thickness than that of the pure components. This fact reveals, somehow, the existence of different interactions between the components of the film when they are mixed rather than when

they are pure. At higher surface pressures, $>30 \text{ mN/m}$, small circular domains are grouped together to result in compact masses of material (Figure 6C), similar to those shown in the images of pure lysozyme when it begins to collapse (Figure 4C). Finally, when the compression is finished, the d – π curve shows the presence of noise peaks of high intensity caused by the presence of a mixed collapsed film (Figure 6D).

3.4.2. Mixed Monolayer of $X_{\text{PMMA}} = 0.4$. Thickness (d) versus surface pressure (π) curves corresponding to the mixed monolayer with composition $X_{\text{PMMA}} = 0.4$, together with the corresponding curves for pure components, are shown in Figure 7, where it can be observed that from the beginning of compression

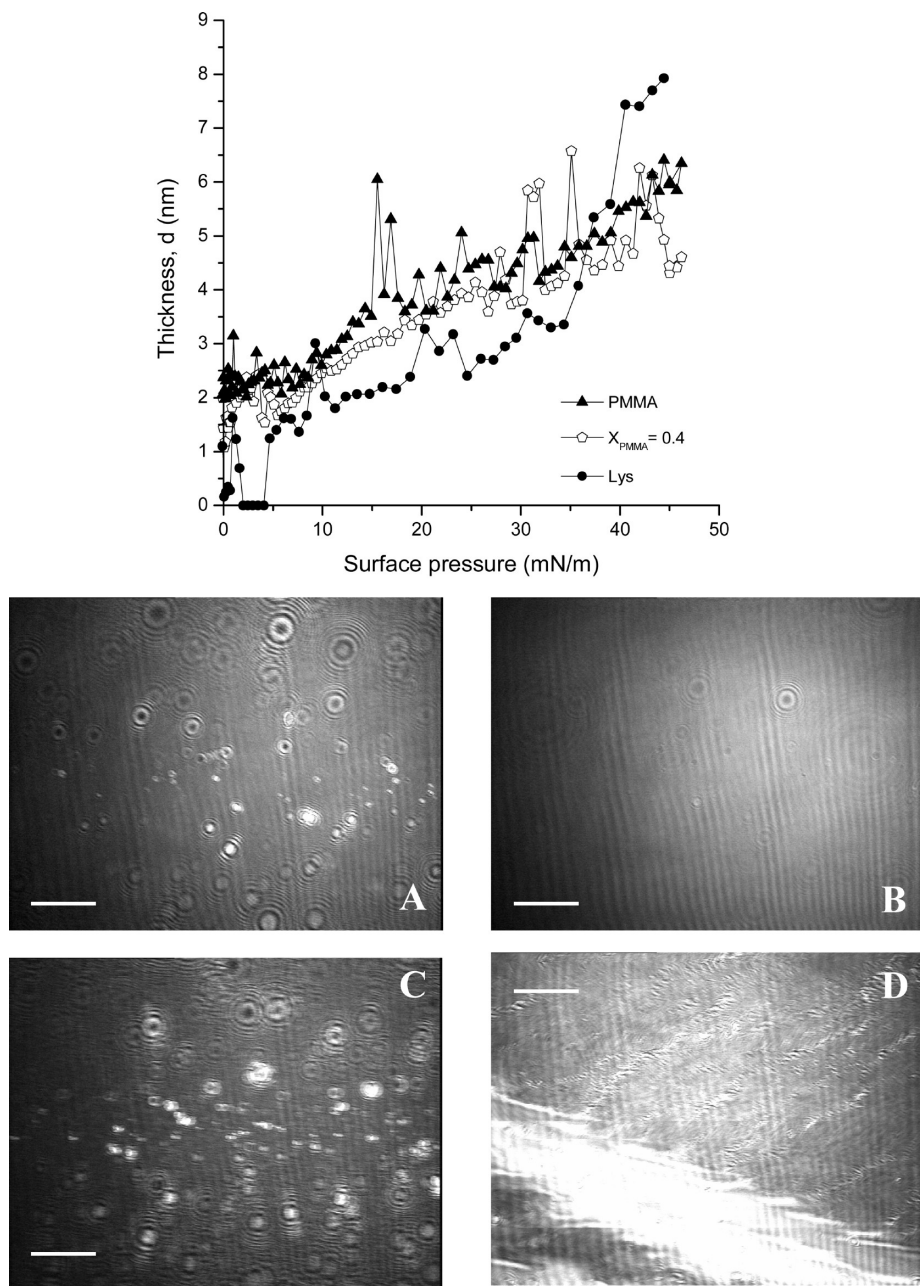


Figure 7. Thickness versus surface pressure plots corresponding to pure and PMMA–lysozyme mixed monolayer of composition $X_{PMMA} = 0.4$ and BAM images obtained at different surface pressure values: (A) $\pi = 0$ mN/m. (B) $\pi = 17.8$ mN/m. (C) $\pi = 32.5$ mN/m. (D) $\pi = 40$ mN/m. Scale bar: 20 μ m.

the relative thickness of the mixed monolayer is more or less constant, ~ 2 nm. In this situation, the BAM images obtained are similar to those recorded in the mixture of $X_{PMMA} = 0.2$ under the same conditions (compare Figure 7A with Figure 6A,B), which were attributed to lysozyme molecules in the mixture. When the mixed film reaches a surface pressure of 10 mN/m, its thickness progressively increases with compression, although the thickness values are lower than those of the pure polymer monolayer but higher than that of lysozyme (Figure 7). This is an intermediate behavior between those of the pure components. In this region, there are no significant noise peaks, which is confirmed by the corresponding homogeneous BAM images (Figure 7B). At surface pressures >30 mN/m, noise peaks reappear in the

thickness curve, the BAM image showing (Figure 7C) the existence of numerous bright domains responsible for the noise. Finally, at the surface pressure of 40 mN/m, the collapse of the mixed monolayer is attained, and masses of high reflectivity appear in BAM images, as shown in Figure 7D.

3.4.3. Mixed Monolayer of $X_{PMMA} = 0.6$. The thickness of the monolayer is higher than that of the pure lysozyme, showing in the thickness versus surface pressure curve the existence of numerous noise peaks with high intensity (Figure 8), which, at low surface pressures, become more important than in the case of PMMA.

In the same way as in the case of the polymer, the thickness of the mixture increases continuously as the monolayer is compressed.

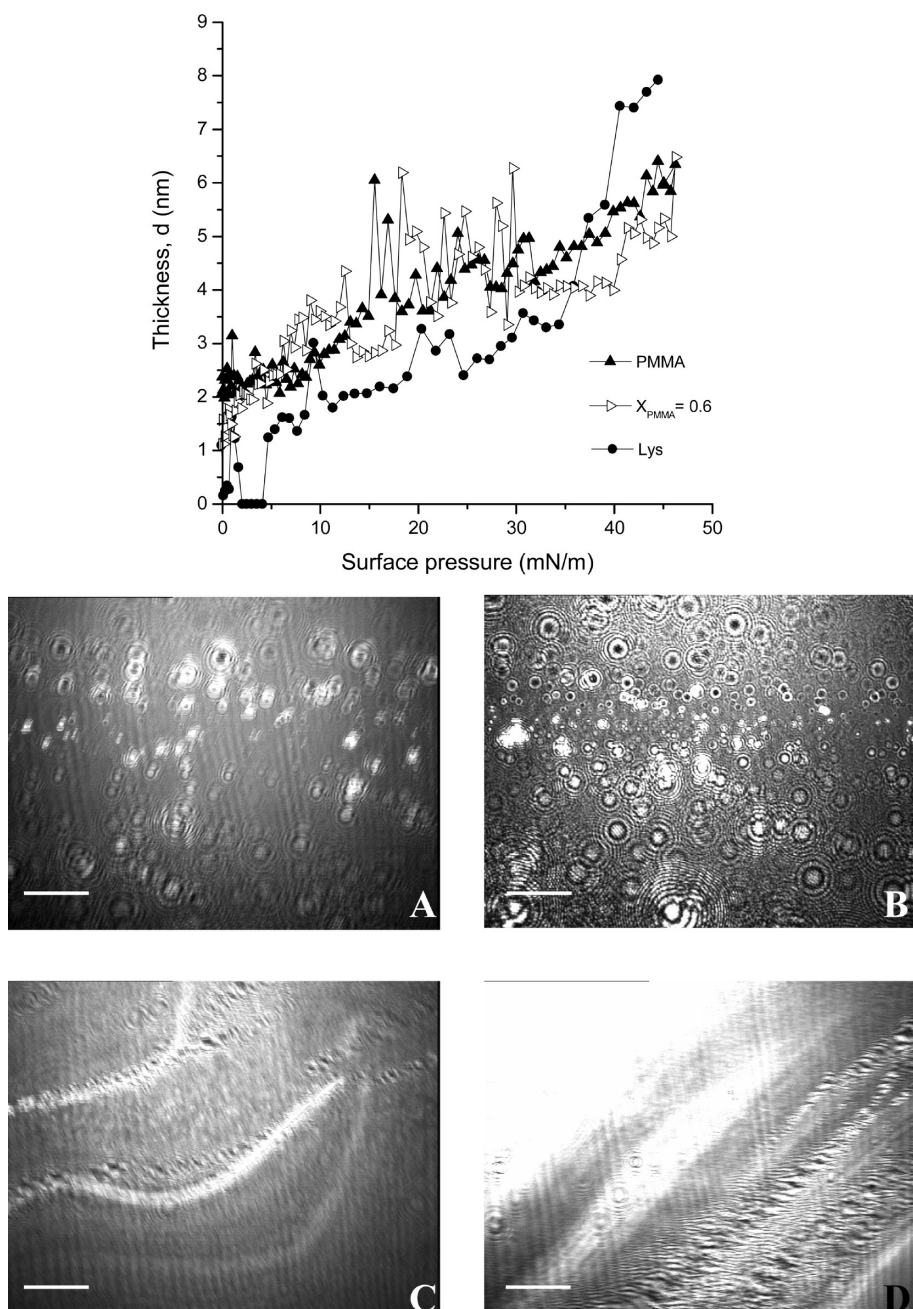


Figure 8. Thickness versus surface pressure plots corresponding to pure and PMMA–lysozyme mixed monolayer of composition $X_{\text{PMMA}} = 0.6$ and BAM images obtained at different surface pressure values: (A) $\pi = 20 \text{ mN/m}$. (B) $\pi = 34.5 \text{ mN/m}$. (C) $\pi = 39 \text{ mN/m}$. (D) $\pi = 45.7 \text{ mN/m}$. Scale bar: $20 \mu\text{m}$.

Above 15 mN/m, there is a sharp increase in thickness, which is attributable to the phase transition of the monolayer under these conditions. After this region, the increase in thickness with compression is continuous again, and the corresponding BAM images show the presence of small circular domains of high reflectivity (white domains) (Figure 8A, obtained at $\pi = 20 \text{ mN/m}$), similar to those of the protein at the surface pressure of 23.5 mN/m (Figure 4B) and to those of the polymer at 17 mN/m (Figure 5A). In view of this, we can say that the BAM images obtained in this region of the isotherm do not differentiate whether the behavior of the monolayer is determined by the polymer or by the protein, which, moreover, is logical taking into

account that in this mixture the proportion of the components is nearly equal (60% PMMA versus 40% of lysozyme). However, at higher surface pressures, $>30 \text{ mN/m}$, the BAM image of the mixture (Figure 8B), obtained at 34.5 mN/m, is similar to that of PMMA recorded at 39 mN/m (Figure 5B). This behavior suggests that the monolayer in this region is formed by the polymer and the collapsed protein, due to the fact that the lysozyme begins to be expelled from the mixed monolayer when the surface pressure reaches 30 mN/m. The BAM image at 39 mN/m (Figure 8C) shows “stripes” of high reflectivity, which are characteristic of the collapse of lysozyme. These clear “stripes”, alternating with other darker ones, show a monolayer configuration in

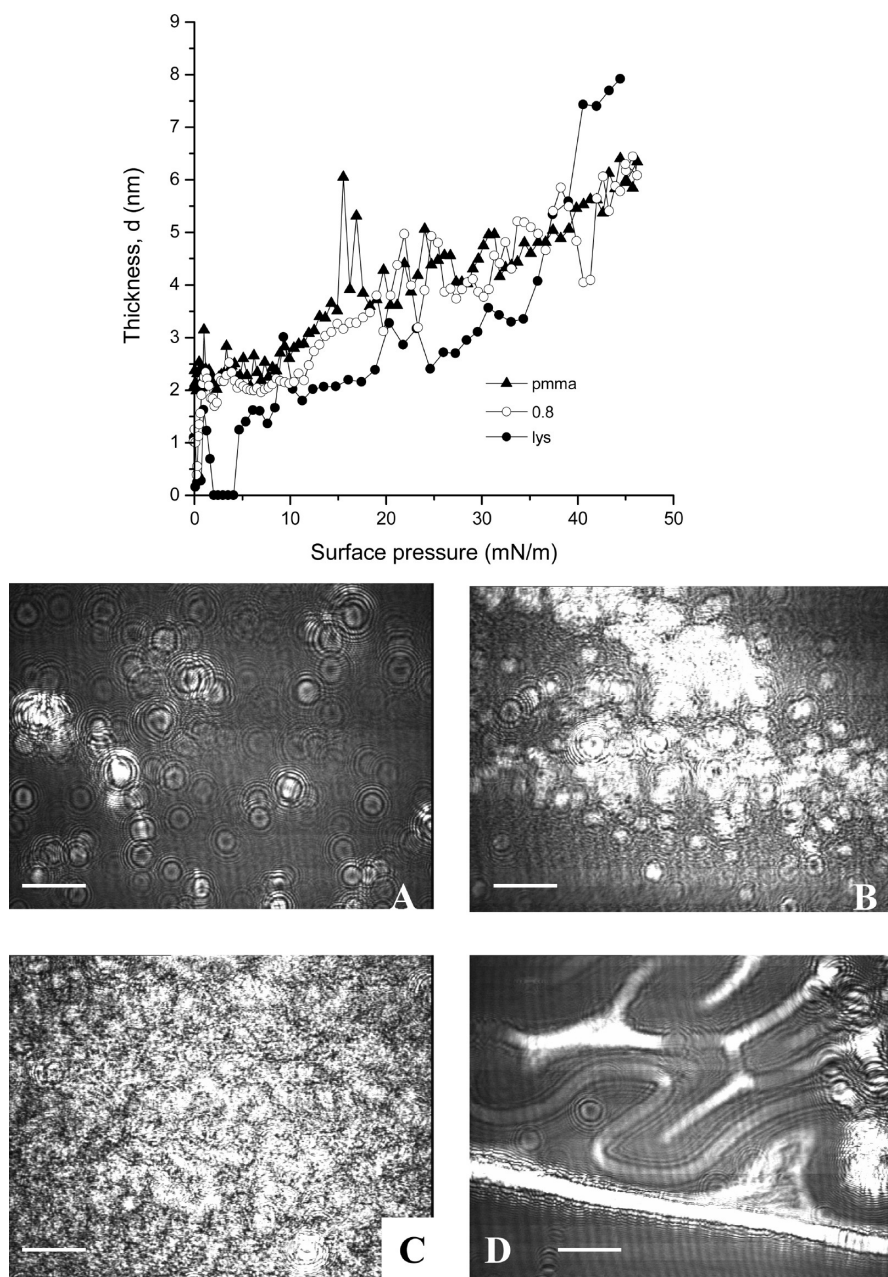


Figure 9. Thickness versus surface pressure plots corresponding to pure and PMMA–lysozyme mixed monolayer of composition $X_{PMMA} = 0.8$ and BAM images obtained at different surface pressure values: (A) $\pi = 17.5$ mN/m. (B) $\pi = 23$ mN/m. (C) $\pi = 38$ mN/m. (D) $\pi = 47$ mN/m. Scale bar: 20 μ m.

“waves” form, as it corresponds to the structure of the protein forming “loops” during the collapse.^{27,28} At higher surface pressures, ~ 45 mN/m, the white “masses” of high reflectivity that appear in the BAM images of the mixture (Figure 8D) correspond to the collapse of PMMA.

3.4.4. Mixed Monolayer of $X_{PMMA} = 0.8$. From 20 mM/m, the thickness versus surface pressure curve for the mixture with composition $X_{PMMA} = 0.8$ (Figure 9) shows the existence of noise peaks, similar to those of the pure PMMA. Along the compression, the mixed monolayer thickness is higher than that of lysozyme, reaching a value close to 6.5 nm when the collapse is achieved. BAM images only show PMMA domains as a result of the excess of this component in the mixture, masking images of lysozyme. The PMMA domains are observed at the beginning

in a more-or-less isolated way (Figure 9A), making up groups as the monolayer is compressed (Figure 9B). Once the surface pressure corresponding to the beginning of the lysozyme collapse (30 mN/m) is exceeded, these domains are still observed, although they are much more compact (Figure 9C). Finally, at higher surface pressures, ~ 47 mN/m, it can be observed that the characteristic protein “folds”, together with white “masses” (Figure 9D) of PMMA, collapsed.

4. DISCUSSION

The analysis of the behavior for PMMA–lysozyme mixed monolayers shows the existence of negative deviations from the additivity of the molecular areas (A_m) when the composition of

polymer mixtures is less than X_{PMMA} 0.6 (Figure 3), regardless of the surface pressure of the monolayers. Above this composition, the experimental A_m values coincide with those calculated from the additivity rule.

The phase diagram shown in Figure 10, carried out using the data in Table 1, describes the macroscopic behavior of the mixed system as it is compressed. Two different situations are considered to analyze the diagram.

4.1. Mixed Monolayers with Composition below to $X_{\text{PMMA}} 0.6$. In this case, the application of the Crisp phase rule^{29,30} ($P = C - F + 1$) to the LE-L'E phase transition ($a-b$ line), where the number of components, C , is 2 and the surface pressure corresponding to the transition (π_{trans}) varies with the composition (so, the degrees of freedom are $F = 1$), proves the existence of two surface phases, P , in equilibrium along the cited $a-b$ line of the phase diagram:

- a) Below the coexistence of the $a-b$ line, mixed monolayer components are horizontally oriented on the water surface, making up "complexes" with a given stoichiometry and constituting a unique homogeneous phase M.
- b) Above the $a-b$ line, PMMA molecules are not fully extended on the water surface, but they are in a more-or-less folded configuration, forming "loops" at the interface.²² This polymer configuration ($\text{PMMA}_{(l)}$) leads to the fact that the system shows an M' phase that is different from the previous phase because the "molecular complex" formed has different characteristics.

When the Crisp phase rule is applied to the phase transition corresponding to the mixed films collapse ($c-d$ line), two phases, P , in equilibrium are obtained. (Because $F = 1$ as a result of that, the collapse surface pressure varies linearly with the mixed film composition.) These are the above-described M' phase and the collapsed phase (M_{collap}) formed by the two collapsed components, constituting a single solid phase.

4.2. Mixed Monolayers with Composition above to X_{PMMA} 0.6. In this case, the LE-L'E transition surface pressure is independent of the mixed film composition ($e-f$ line), so $F = 0$ and $P = 3$. The three phases are: (a) pure lysozyme, segregated from the polymer as a result of the fact that a high proportion of the latter is not adequate to make up the above-described complex; (b) $\text{PMMA}_{(h)}$ molecules, horizontally oriented on the water surface; and (c) PMMA "loops", ($\text{PMMA}_{(l)}$).

At surface pressures above the LE-L'E phase, the mixed monolayers show two collapses: the first, at a surface pressure of $\sim 30 \text{ mN/m}$ ($g-h$ line), corresponds to the lysozyme segregation from the mixed film, and the second, at higher surface pressures, $\sim 47.5 \text{ mN/m}$ ($i-j$ line), corresponds to the PMMA collapse. By applying the Crisp phase rule to the first collapse, where $F = 0$ (collapse surface pressure is independent of composition), we obtained $P = 3$; namely, along the $g-h$ line there are three phases in equilibrium formed by: (a) $\text{PMMA}_{(l)}$, (b) uncollapsed lysozyme ($\text{lysozyme}_{(h)}$), and (c) collapsed protein ($\text{lysozyme}_{(\text{coll})}$). Similarly, along the $i-j$ line, there are also three phases in equilibrium, namely: collapsed lysozyme, ($\text{lysozyme}_{(\text{coll})}$), $\text{PMMA}_{(l)}$, and collapsed PMMA ($\text{PMMA}_{(\text{collap})}$).

In short, mixed monolayers of lysozyme and PMMA have two different macroscopic behaviors depending on their composition: at low PMMA concentrations, the components make up a miscible system with negative deviations from the ideal behavior, whereas at high concentrations the components are segregated from the mixed system constituting an immiscible system.

4.3. Molecular Interpretation of the PMMA–Lysozyme Interaction. The existence of negative deviations from the ideal

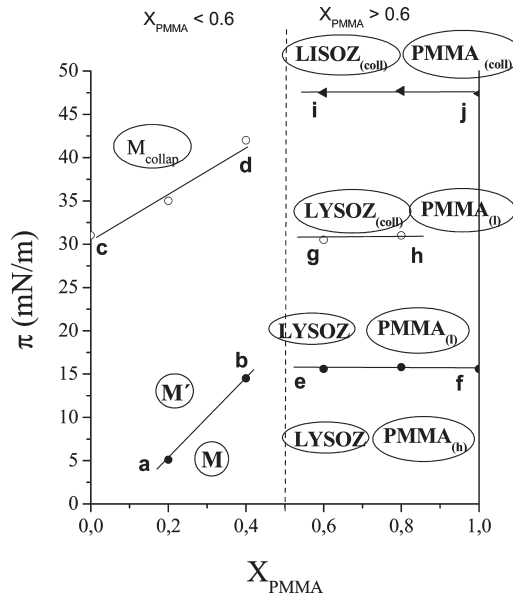


Figure 10. Phase diagram corresponding to PMMA–lysozyme mixed monolayers obtained from data of Table 1.

behavior, with a minimum in $A-X_{\text{PMMA}}$ plots at mole fraction $X_{\text{PMMA}} = 0.25$ (Figure 3), proves that the attractive molecular forces between the mixed components are greater than those when they are pure. Traditionally, in the literature, there are different theories to explain the nature of these negative deviations from the ideal behavior. Many authors referred in the past to the formation of complex or molecular aggregates with a certain stoichiometry at "definite proportions", in which hydrogen bonds, dipole–dipole or ion–dipole attractive forces between polar groups are predominant.³¹ More recently,³² the formation of molecular complexes of 1:1 and 2:1 stoichiometry has been suggested to explain the negative deviations from the ideal behavior for cholesterol/oleic acid/linoleic acid mixed systems, attributed to van der Waals attractive forces between cholesterol rings and aliphatic chains of fatty acids. In this same sense, Zhao and Feng^{33–35} postulate that the condensing action of paclitaxel on phospholipid monolayers is due to geometrical accommodation of the components in the mixed films, as a result of the strong van der Waals forces between alkyl chains. Moreover, Fukuda et al.³⁶ attribute the negative deviations of poly(vinyl stearate)–hexadecanol mixed films to the packing of these compounds. In the same line, our studies on amphotericin B (AmB)–phospholipids^{37–41} and AmB–cholesterol^{42,43} mixed films confirm the existence of a complex 2:1 (AmB/phospholipid or AmB/cholesterol), via the formation of hydrogen bonds between hydroxyl groups of the phospholipid (or cholesterol) and AmB, respectively, and via ionic interactions between the ionized phosphate groups of phospholipids and the positively charged groups of AmB, which explains the deviations from the ideal behavior of these systems.

Taking into account this background, it can be speculated that the strong negative deviation from the ideal behavior of the lysozyme–PMMA mixed system with $X_{\text{PMMA}} = 0.25$ (Figure 3) can be due to the formation of a complex consisting of one polymer molecule and three molecules of protein (1:3 stoichiometry), stabilized by hydrogen bonds between the NH groups of the protein and the CO groups of the polymer as well as by van der

Waals attractive forces between the hydrocarbon chains of both components. Attractive electrostatic (ionic) molecular interactions between these components could be ruled because PMMA is an uncharged polymer and lysozyme is spread on the subphase at a pH near their isoelectric point, that is, with a net electrical charge close to zero. Nevertheless, it is possible that the existence of electrostatic interactions between the charges of the protein and the Na^+ (and Cl^-) ions at the air/water interface is a result of using a substrate of high ionic strength (NaCl 3M). In other substrates with low saline concentration, or water, significant changes in the mean molecular areas and, consequently, in the stoichiometry of the complex, could take place. However, is not possible to check this effect because under different conditions from those used in this study (i.e., at different pH and ionic strength of the substrate, among others), the lysozyme is not fully spread at the interface because there is a significant loss of protein caused by their desorption or dissolution into the subphase.

When the relative proportion of the components in the mixed film differs significantly from the value corresponding to the stoichiometry of the complex (as in mixtures with $X_{\text{PMMA}} > 0.6$), this complex cannot be formed, causing an immiscible system where the values of the experimental molecular area coincide with those corresponding to the ideal behavior.

5. CONCLUSIONS

Mixed monolayers of PMMA and lysozyme show two different macroscopic behaviors depending on their composition. At low PMMA concentrations ($X_{\text{PMMA}} = 0.2$ and 0.4), the film components form a miscible system where the surface pressure corresponding to the LE-L'E phase transition and the collapse pressure of the mixed films vary with the composition of the mixtures. In this region, the mean molecular area versus mole fraction plots show the existence of negative deviations from ideality, with a maximum deviation in the mixed monolayer with composition $X_{\text{PMMA}} \approx 0.25$. This behavior can be attributed to the possible formation of a complex consisting of one polymer molecule and three molecules of protein (1:3 stoichiometry).

At high PMMA concentrations ($X_{\text{PMMA}} = 0.6$ and 0.8), the surface pressure corresponding to the LE-L'E phase transition of the mixed films does not vary with its composition. The mixed monolayers show two collapses: a first corresponding to the lysozyme segregation from the mixture and a second, at higher surface pressures, corresponding to the PMMA. Also, the experimental values of the mean molecular area of the mixed monolayers in this region match up virtually with the theoretical values calculated from the additivity rule. All of these results are typical of mixed films formed by immiscible components at the air/water interface. Consequently, when the relative proportion of the components in the mixed films significantly differs from the value corresponding to the stoichiometry of the complex (as in mixtures with $X_{\text{PMMA}} > 0.6$), this complex cannot be formed, causing an immiscible system.

Measurements of monolayer thickness and BAM images allow us to confirm on microscopic level the structural characteristics deduced from the π -A isotherms.

AUTHOR INFORMATION

Corresponding Author

*Phone: +34 981 563100, ext. 14917. Fax: +34 981 594912.
E-mail: qf.minones@usc.es.

ACKNOWLEDGMENT

We acknowledge the support of Xunta de Galicia (Spain) through the project number PGIDIT07PXIB203133PR.

REFERENCES

- (1) Adler, F. H.; Alm, A. Chapter 2. In *Fisiología del Ojo: Aplicación Clínica*; Elsevier: Madrid, Spain, 2003; pp 28–39.
- (2) Tanford, C.; Wagner, M. L. *J. Am. Chem. Soc.* **1954**, *76*, 3331.
- (3) Powrie, W. D. Y.; Nakai, S. Chapter 14. In *Química de los Alimentos*; Fennema, O., Ed.; Acribia: Zaragoza, Spain, 2000; pp 931–959.
- (4) Blake, C. C. F.; Koenig, D. F.; Mair, G. A.; North, A. C. T.; Phillips, D. C.; Sarma, V. R. *Nature* **1965**, *757*, 206.
- (5) Haggerty, C. Doctoral Thesis, University of Aston: Birmingham, U.K., 1971; p 1953.
- (6) Barnett, E. V. *J. Immunol.* **1968**, *100*, 1093.
- (7) Sapse, A.; Bonavide, B.; Stone, W.; Sercarz, E. *Am. J. Ophthalmol.* **1968**, *66*, 76.
- (8) Sastre, R.; Mateo, J. L. *Rev. Plast. Mod.* **1988**, *379*, 77.
- (9) Maget-Dana, R. *Biochim. Biophys. Acta* **1999**, *1462*, 109.
- (10) Stallberg, S.; Theorell, T. *Trans. Faraday Soc.* **1939**, *35*, 1413.
- (11) Crisp, D. J. *J. Colloid Sci.* **1946**, *1*, 161.
- (12) Beredjick, N.; Ahlbeck, R. A.; Kwei, T. K.; Ries, H. E., Jr. *J. Polym. Sci.* **1960**, *46*, 268.
- (13) Hsu, W. P.; Lee, Y. L.; Liou, S. H. *Appl. Surf. Sci.* **2006**, *252*, 4312.
- (14) Gaines, G. L., Jr. *Insoluble Monolayers at Liquid-Gas Interface*; Prigogine, I., Ed.; Interscience: New York, 1966; pp 269–270.
- (15) Trunxit, H. T. *J. Colloid Sci.* **1960**, *15*, 1.
- (16) Muramatsu, S.; Sobotka, H. *J. Phys. Chem.* **1962**, *66*, 1918.
- (17) Miñones, J.; Iribarne, E.; García Fernández, S.; Sanz Pedrero, P. *Kolloid Z. Z. Polym.* **1972**, *250*, 318. *1972*, *250*, 325.
- (18) Miñones, J.; Conde, O.; Gómez-Ulla, A. *Colloids Surf.* **1984**, *10*, 85.
- (19) Casas, M.; Miñones, J.; Iribarne, E. *Colloids Surf.* **1991**, *59*, 345.
- (20) Casas, M.; Miñones, J. *Colloid Polym. Sci.* **1992**, *270*, 478. *1992*, *270*, 842.
- (21) Miñones, M.; Conde, O.; Trillo, J. M.; Miñones, J. *Colloid Interface Sci.* **2011** accepted for publication.
- (22) Miñones, J.; Miñones Conde, M.; Yebra-Pimentel, E.; Trillo, J. M. *J. Phys. Chem.* **2009**, *113*, 17455.
- (23) Rodríguez Patino, J. M.; Carrera, C.; Rodríguez Niño, M. R. *Langmuir* **1999**, *15*, 2484.
- (24) Gilardoni, A.; Margheri, E.; Gabrielli, G. *Colloids Surf.* **1992**, *68*, 235.
- (25) Bonosi, F.; Margheri, E.; Gabrielli, G. *Colloids Surf.* **1992**, *65*, 287.
- (26) Petrov, J. G.; Möbius, D.; Angelova, A. *Langmuir* **1992**, *8*, 201.
- (27) Rodríguez Niño, M. R.; Carrera, C.; Rodriguez Patino, J. M. *Colloids Surf.* **1999**, *12*, 161.
- (28) Rodríguez Patino, J. M.; Rodríguez Niño, M. R.; Carrera, C. *Langmuir* **2002**, *18*, 8455.
- (29) Crisp, D. J. *Surface Chemistry (Supplement Research)*; Butterworth: London, 1949; pp 17–35.
- (30) Defay, R.; Prigogine, I.; Bellmans, A.; Everett, D. E. *Surface Tension and Adsorption*; Longmans Green and Co.: London, 1966; p 71.
- (31) Dervichian, D. G. *Surface Phenomena in Chemistry and Biology*; Danielli, J. F., Pankhurst, K. G. A., Riddiford, A. C., Ed.; Pergamon Press: London, 1958; pp 70–88.
- (32) Seoane, R.; Miñones, J.; Conde, O.; Miñones, J., Jr.; Casas, M.; Iribarne, E. *J. Phys. Chem. B* **2000**, *104*, 7735.
- (33) Zhao, L.; Feng, S. S.; Go, M. L. *J. Pharm. Sci.* **2004**, *93*, 86.
- (34) Zhao, L.; Feng, S. S. *J. Colloid Interface Sci.* **2004**, *274*, 55.
- (35) Zhao, L.; Feng, S. S. *J. Colloid Interface Sci.* **2005**, *285*, 326.
- (36) Fukuda, K.; Kato, T.; Machida, S.; Shimizu, Y. *J. Colloid Interface Sci.* **1979**, *68*, 82.

- (37) Miñones, J., Jr; Miñones, J.; Conde, O.; Seoane, R.; Dynarowick-Latka, P. *Langmuir* **2000**, *16*, 5743.
- (38) Miñones, J., Jr.; Conde, O.; Miñones, J.; Rodríguez Patino, J. M.; Seoane, R. *Langmuir* **2002**, *18*, 8601.
- (39) Miñones, J., Jr; Miñones, J.; Conde, O.; Rodríguez Patino, J. M.; Dynarowick-Latka, P. *Langmuir* **2002**, *18*, 2817.
- (40) Miñones, J., Jr.; Dynarowick-Latka, P.; Conde, O.; Miñones, J.; Iribarnegaray, E.; Casas, M. *Colloids Surf, B* **2003**, *29*, 205.
- (41) Miñones, J., Jr; Miñones, J.; Rodríguez Patino, J. M.; Conde, O.; Iribarnegaray, E. *J.Phys. Chem. B* **2003**, *107*, 4189.
- (42) Seoane, R.; Conde, O.; Casas, M.; Iribarnegaray, E. *Biochim. Biophys. Acta* **1375**, *73*, 1998.
- (43) Seoane, R.; Miñones, J.; Conde, O.; Casas, M.; Iribarnegaray, E. *Langmuir*. **1999**, *15*, 3570. *1999*, *15*, 5567.